

The protective roles of GLP-1R signaling in diabetic nephropathy: possible mechanism and therapeutic potential

Hiroki Fujita¹, Tsukasa Morii¹, Hiromi Fujishima¹, Takehiro Sato¹, Tatsunori Shimizu¹, Mihoko Hosoba¹, Katsushi Tsukiyama¹, Takuma Narita¹, Takamune Takahashi², Daniel J. Drucker^{3,4}, Yutaka Seino⁵ and Yuichiro Yamada¹

¹Division of Endocrinology, Metabolism and Geriatric Medicine, Akita University Graduate School of Medicine, Akita, Japan; ²Division of Nephrology and Hypertension, Vanderbilt University Medical Center, Nashville, Tennessee, USA; ³Department of Medicine, University of Toronto, Toronto, Ontario, Canada; ⁴The Lunenfeld-Tanenbaum Research Institute, Mt Sinai Hospital, Toronto, Ontario, Canada and ⁵Kansai Electric Power Hospital, Osaka, Japan

Glucagon-like peptide-1 (GLP-1) is a gut incretin hormone that has an antioxidative protective effect on various tissues. Here, we determined whether GLP-1 has a role in the pathogenesis of diabetic nephropathy using nephropathy-resistant C57BL/6-Akita and nephropathy-prone KK/Ta-Akita mice. By *in situ* hybridization, we found the GLP-1 receptor (GLP-1R) expressed in glomerular capillary and vascular walls, but not in tubuli, in the mouse kidney. Next, we generated C57BL/6-Akita *Glp1r* knockout mice. These mice exhibited higher urinary albumin levels and more advanced mesangial expansion than wild-type C57BL/6-Akita mice, despite comparable levels of hyperglycemia. Increased glomerular superoxide, upregulated renal NAD(P)H oxidase, and reduced renal cAMP and protein kinase A (PKA) activity were noted in the *Glp1r* knockout C57BL/6-Akita mice. Treatment with the GLP-1R agonist liraglutide suppressed the progression of nephropathy in KK/Ta-Akita mice, as demonstrated by reduced albuminuria and mesangial expansion, decreased levels of glomerular superoxide and renal NAD(P)H oxidase, and elevated renal cAMP and PKA activity. These effects were abolished by an adenylate cyclase inhibitor SQ22536 and a selective PKA inhibitor H-89. Thus, GLP-1 has a crucial role in protection against increased renal oxidative stress under chronic hyperglycemia, by inhibition of NAD(P)H oxidase, a major source of superoxide, and by cAMP-PKA pathway activation.

Kidney International advance online publication, 23 October 2013; doi:10.1038/ki.2013.427

KEYWORDS: diabetic nephropathy; glucagon-like peptide-1; oxidative stress

Correspondence: Hiroki Fujita, Division of Endocrinology, Metabolism and Geriatric Medicine, Akita University Graduate School of Medicine, 1-1-1 Hondo, Akita 010-8543, Japan. E-mail: hirofujii@gipc.akita-u.ac.jp

Received 5 February 2013; revised 8 September 2013; accepted 12 September 2013

Diabetic nephropathy (DN) is a serious complication of diabetes and the leading cause of end-stage renal disease in developed countries. Recent evidence indicates that oxidative stress has a central role in the development and progression of DN.^{1,2} The increase in systemic oxidative stress becomes prominent from the incipient stage of DN.³ In the kidney, reactive oxygen species (ROS) including superoxide anion ($O_2^{\bullet-}$) are excessively produced by chronic hyperglycemia, leading to increased levels of renal oxidative stress. NAD(P)H oxidase is the most important source of superoxide anion,⁴⁻⁷ and this enzyme is shown to be upregulated in the diabetic kidney.^{5,8-10} A recent *in vitro* study using human HEK293 cells demonstrated that NAD(P)H oxidase NOX1-dependent ROS production is reduced by the elevation of cAMP and subsequent activation of protein kinase A (PKA).¹¹ Furthermore, treatment with cAMP-elevating agents such as isoproterenol and forskolin normalized the levels of NAD(P)H oxidase activity and superoxide in aortic vascular smooth muscle cells of spontaneously hypertensive rats.¹² Thus, the cAMP-PKA pathway appears to work as an important inhibitory factor for NAD(P)H oxidase-dependent production of ROS or superoxide.

Glucagon-like peptide-1 (GLP-1) is a gut incretin hormone that stimulates insulin secretion from pancreatic β -cells in a glucose-dependent manner.¹³ Activation of the GLP-1 receptor (GLP-1R) stimulates adenylate cyclase and enhances the production of cAMP, the primary effector of GLP-1-induced insulin secretion.^{13,14} Furthermore, increased levels of cAMP activate PKA or cAMP-regulated guanine nucleotide exchange factor II (Epac2), and contribute to mediating various physiological actions including insulin secretion.^{14,15} The GLP-1R is expressed in pancreatic β -cells and in multiple extrapancreatic tissues including the gut, brain, heart, lung, and kidney.^{16,17} Given the evidence indicating that cAMP and PKA pathways link to antioxidative effects, it is likely that GLP-1 protects various tissues from oxidative injury. However, the roles of GLP-1 in the kidney and DN have not been fully

elucidated. First, the precise localization of GLP-1R in the kidney remains unclear. Second, it is unknown whether gain or loss of GLP-1R signaling modulates renal function and the progression of renal injury under conditions of chronic hyperglycemia.

In the present study, we investigated the role of endogenous GLP-1R signaling in DN. First, we examined the localization of GLP-1R in the mouse kidney by *in situ* hybridization and reverse transcriptase polymerase chain reaction (RT-PCR) analysis. Next, we studied two *Ins2^{Akita}* diabetic mouse models showing different susceptibility to the development and progression of DN, DN-resistant C57BL/6-*Ins2^{Akita}* (C57BL/6-Akita), and DN-prone KK/Ta-*Ins2^{Akita}* (KK/Ta-Akita).^{18,19} We examined the renal phenotypes of C57BL/6-Akita mice with GLP-1R deficiency, and in complementary experiments, we tested whether a GLP-1R agonist, liraglutide, ameliorates nephropathic changes in KK/Ta-Akita mice that develop progressive DN.¹⁸

RESULTS

Renal expression and localization of the *Glp1r* in mice

As recent studies have highlighted the lack of sensitivity and specificity of multiple GLP-1R antisera,^{20,21} we used *in situ* hybridization analysis to assess *Glp1r* expression in kidneys of 8-week-old male C57BL/6-wild-type (C57BL/6-WT) mice. As shown in Figure 1, *Glp1r* mRNA transcripts were localized along glomerular capillary walls and throughout vascular walls, but not in tubules and collecting ducts, in the kidney. In particular, the *in situ* hybridization analysis revealed that the *Glp1r* is predominantly expressed in renal blood vessels. To further verify these findings, we examined *Glp1r* mRNA expression in isolated enriched preparations of glomeruli, tubuli, and renal arteries. Consistent with the results of *in situ* hybridization analysis, *Glp1r* mRNA transcripts were detected in RNA from glomeruli and to a greater extent in renal arteries, but not in tubuli (Figure 1e and f).

Generation of GLP-1R- and insulin-deficient C57BL/6-Akita mice and basic metabolic measurements

We next confirmed the lack of *Glp1r* expression in newly generated lines of Akita mice lacking the *Glp1r*. Figure 2a shows the data of RT-PCR analysis in 30-week-old GLP-1R-deficient C57BL/6 strain mice (*Glp1r^{-/-}*) and GLP-1R-present littermates (*Glp1r^{+/+}*). A complete absence of renal glomerular *Glp1r* mRNA was confirmed in *Glp1r^{-/-}* mice. The levels of glomerular *Glp1r* mRNA transcripts were similar between nondiabetic C57BL/6-WT and diabetic C57BL/6-Akita mice. As shown in Figure 2b, GLP-1R deficiency did not affect islet topography and the number of insulin+ cells in the C57BL/6-Akita mice. Table 1 shows biochemical and physiological parameters at 30 weeks of age in the WT and Akita *Glp1r^{-/-}* and *Glp1r^{+/+}* mice. GLP-1R deficiency did not affect plasma levels of active GLP-1, glucose, and insulin. Furthermore, there were no significant differences in body weight, systolic blood pressure, blood urea nitrogen, and plasma lipids between *Glp1r^{+/+}* and

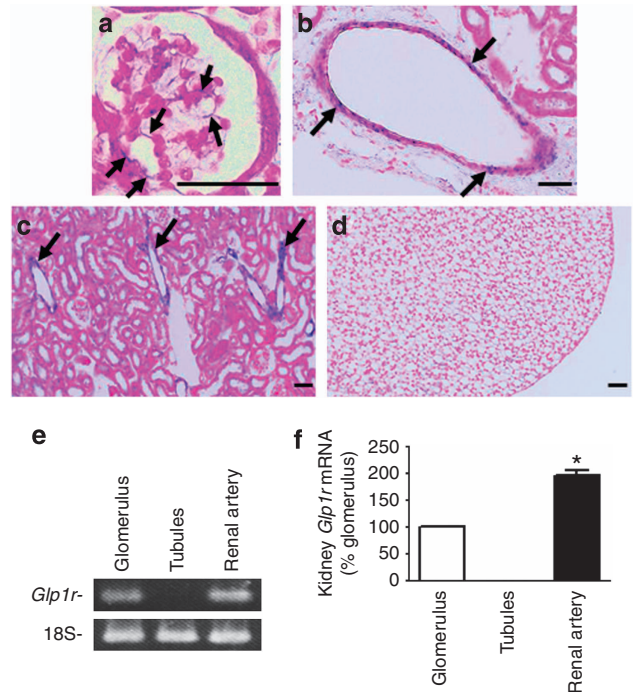


Figure 1 | Analysis of kidney *Glp1r* mRNA expression.

Representative *in situ* hybridization images of *Glp1r* mRNA expression are shown in upper panels. (a) Glomerulus, (b) blood vessel, (c) cortex, and (d) papilla in 8-week-old male C57BL/6-WT mouse kidney. Arrows indicate *Glp1r* mRNA expression. Bars = 50 μm. (e and f) Lower panels show the results of reverse transcriptase polymerase chain reaction (PCR) analysis in glomeruli, tubuli, and renal arteries isolated from 8-week-old male C57BL/6-WT mouse kidneys (n = 5 per group; *P < 0.001 vs. glomerulus).

Glp1r^{-/-} C57BL/6-Akita mice. Interestingly, *Glp1r^{-/-}* C57BL/6-Akita mice exhibited significantly higher levels of urinary albumin, glomerular filtration rate (GFR), and kidney weight relative to *Glp1r^{+/+}* C57BL/6-Akita mice. The mild changes in the renal phenotype of *Glp1r^{-/-}* C57BL/6-Akita mice were detected by 15 weeks of age (data not shown), and these mice developed overt renal diabetic changes by 30 weeks of age. In contrast, we did not observe similar changes in renal parameters in *Glp1r^{+/+}* C57BL/6-WT mice.

Renal glomerular histopathology in *Glp1r^{-/-}* C57BL/6-Akita mice

Figure 3 shows glomerular histopathology at 30 weeks of age in *Glp1r^{+/+}* versus *Glp1r^{-/-}* C57BL/6-WT and C57BL/6-Akita mice. Interestingly, periodic acid-Schiff (PAS) staining examination revealed increased mesangial expansion in *Glp1r^{-/-}* C57BL/6-Akita mice as compared with *Glp1r^{+/+}* C57BL/6-Akita mice. Nondiabetic C57BL/6-WT mice displayed normal glomerular histology. Obvious tubulointerstitial injury was not observed in any groups (data not shown). Fibronectin (FN) is an extracellular matrix component and is present along glomerular basement membranes. An increase in FN deposition is observed during glomerular injury,²² and hence FN is used as a marker of diabetic

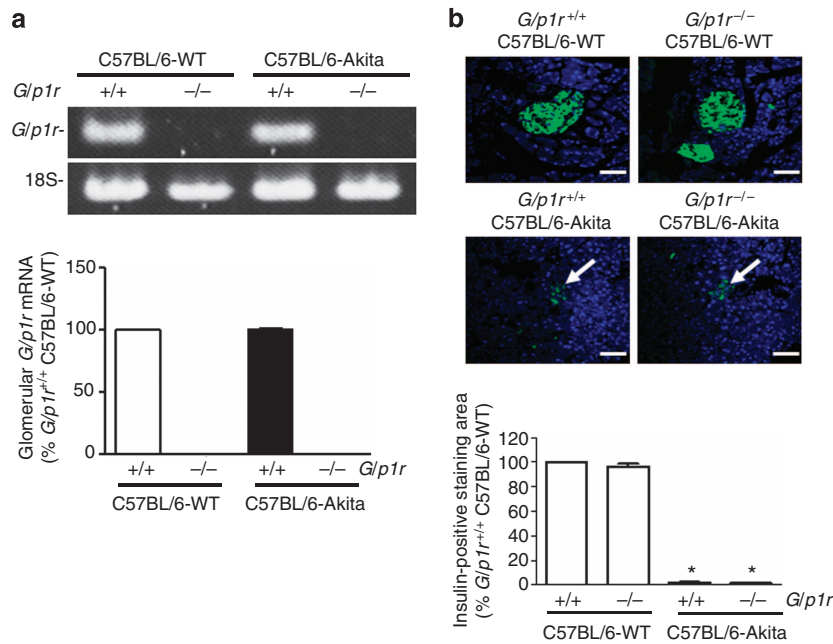


Figure 2 | Generation of glucagon-like peptide-1 receptor (GLP-1R)- and insulin-deficient C57BL/6-Akita mice. (a) Reverse transcriptase polymerase chain reaction (PCR) analysis of glomerular *Glp1r* mRNA expression in 30-week-old male mice. Loss of *Glp1r* mRNA transcripts was confirmed in *Glp1r*^{-/-} mouse glomeruli ($n = 5$ per group). **(b)** Pancreas insulin immunohistochemistry in 30-week-old male mice ($n = 5$ per group; * $P < 0.001$ vs. *Glp1r*^{+/+} C57BL/6-WT). Arrows indicate pancreatic islet. Bars = 50 μ m. WT, wild type.

Table 1 | Biochemical and physiological parameters in 30-week-old male mice

	C57BL/6-WT		C57BL/6-Akita	
	<i>Glp1r</i> ^{+/+}	<i>Glp1r</i> ^{-/-}	<i>Glp1r</i> ^{+/+}	<i>Glp1r</i> ^{-/-}
<i>n</i>	5	10	5	10
BW (g)	30.2 \pm 0.6	28.5 \pm 0.5	23.4 \pm 0.4*	22.0 \pm 0.7*
SBP (mm Hg)	99 \pm 1	99 \pm 1	116 \pm 4 [†]	115 \pm 3 [†]
BG (mg/dl)	153 \pm 5	156 \pm 5	500 \pm 38*	506 \pm 21*
Plasma insulin (ng/ml)	0.63 \pm 0.05	0.54 \pm 0.11	0.09 \pm 0.02*	0.06 \pm 0.02*
Plasma active GLP-1 (pg/ml)	11.7 \pm 2.0	11.2 \pm 2.9	12.1 \pm 2.9	9.3 \pm 2.6
BUN (mg/dl)	20.9 \pm 1.1	20.9 \pm 1.2	34.2 \pm 1.8*	36.7 \pm 1.6*
Cre (mg/dl)	0.74 \pm 0.02	0.70 \pm 0.02	0.84 \pm 0.07	0.83 \pm 0.04
TC (mg/dl)	78.2 \pm 5.0	75.4 \pm 2.4	84.0 \pm 4.4	86.2 \pm 4.6
TG (mg/dl)	123 \pm 5	109 \pm 9	121 \pm 7	113 \pm 13
ACR (μ g/mg creatinine)	9.7 \pm 1.3	10.1 \pm 0.9	50.0 \pm 3.5 [‡]	86.2 \pm 15.6* [§]
GFR (μ l/min/g BW)	10.0 \pm 0.5	10.2 \pm 0.5	16.9 \pm 0.8*	20.1 \pm 0.5*
LKW/BW (g/kg)	5.2 \pm 0.1	6.5 \pm 0.3	9.3 \pm 0.4*	12.9 \pm 0.6*

Abbreviations: ACR, urinary albumin-to-creatinine ratio; BG, blood glucose; BUN, blood urea nitrogen; BW, body weight; Cre, plasma creatinine; GFR, glomerular filtration rate; GLP-1, glucagon-like peptide-1; LKW, left kidney weight; SBP, systolic blood pressure; TC, total cholesterol; TG, triglyceride; WT, wild type. Values are means \pm s.e.m.

* $P < 0.001$, [†] $P < 0.01$, [‡] $P < 0.05$ vs. *Glp1r*^{+/+} C57BL/6-WT; [§] $P < 0.05$, ^{||} $P < 0.01$ vs. *Glp1r*^{+/+} C57BL/6-Akita.

glomerular injury. Compared with *Glp1r*^{+/+} C57BL/6-Akita mice, *Glp1r*^{-/-} C57BL/6-Akita mice displayed significantly increased FN accumulation in glomerular capillary walls (Figure 3a and c). WT1 staining analysis revealed a significant reduction of podocyte number in *Glp1r*^{-/-} C57BL/6-Akita mice relative to *Glp1r*^{+/+} C57BL/6-Akita mice (Figure 3a and d). Furthermore, through electron microscopic analysis, we observed irregular thickening of the glomerular basement membrane (GBM) in *Glp1r*^{-/-} C57BL/6-Akita mice (Figure 3a). Morphometric analysis revealed a significant

increase in GBM thickness in *Glp1r*^{-/-} C57BL/6-Akita mice (Figure 3e).

Renal changes in cAMP and PKA activity levels in *Glp1r*^{-/-} C57BL/6-Akita mice

Figure 4 shows renal cAMP and PKA activity levels at 30 weeks of age in *Glp1r*^{+/+} versus *Glp1r*^{-/-} C57BL/6-WT and C57BL/6-Akita mice. Renal levels of both cAMP and PKA activity were markedly reduced in *Glp1r*^{-/-} C57BL/6-WT and *Glp1r*^{-/-} C57BL/6-Akita mice. In contrast, levels of renal cAMP and PKA activity were similar in *Glp1r*^{+/+} mice. These findings indicate that renal cAMP and PKA activity are regulated by the presence or absence of the *Glp1r*, independent of levels of glycemia in mice.

Renal changes in oxidative stress markers in *Glp1r*^{-/-} C57BL/6-Akita mice

The degree of renal oxidative stress was assessed using dihydroethidium (DHE) histochemistry and thiobarbituric acid-reactive substance (TBARS) assay at 30 weeks of age in *Glp1r*^{+/+} versus *Glp1r*^{-/-} C57BL/6-WT and C57BL/6-Akita mice. As shown in Figure 5a and b, the glomeruli in C57BL/6-Akita diabetic mouse groups showed intense DHE fluorescence, indicating increased glomerular superoxide production. Notably, glomerular DHE fluorescence was stronger in kidneys from *Glp1r*^{-/-} C57BL/6-Akita mice. Renal levels of TBARS, a sensitive marker of oxidative stress, were elevated in C57BL/6-Akita diabetic mouse groups (Figure 5e) and significantly greater in *Glp1r*^{-/-} C57BL/6-Akita mice, suggesting that GLP-1R deficiency contributes to

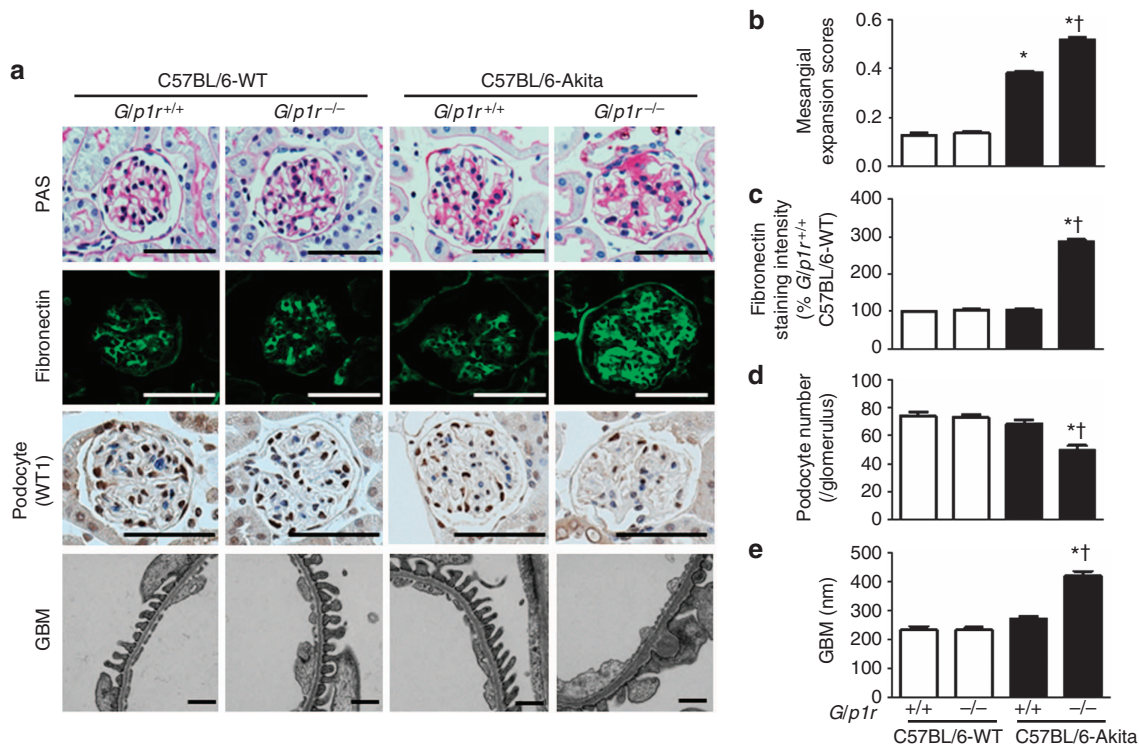


Figure 3 | Renal histopathology in glucagon-like peptide-1 receptor (GLP-1R)-deficient C57BL/6-Akita mice. (a) Representative glomerulus images of periodic acid-Schiff (PAS) staining, fibronectin immunohistochemistry, WT1 staining, and electron microscopic analysis in 30-week-old male mouse kidneys. Bars = 50 μm for PAS, fibronectin, and WT1 images or 1 μm for glomerular basement membrane (GBM) images. (b) Glomerular mesangial expansion scores. (c) Semiquantified fluorescence intensity of glomerular fibronectin. (d) The number of WT1-positive podocytes in the glomeruli. (e) GBM thickness ($n = 5$ per group; $*P < 0.001$ vs. *Glp1r*^{+/+} C57BL/6-WT; $†P < 0.001$ vs. *Glp1r*^{+/+} C57BL/6-Akita).

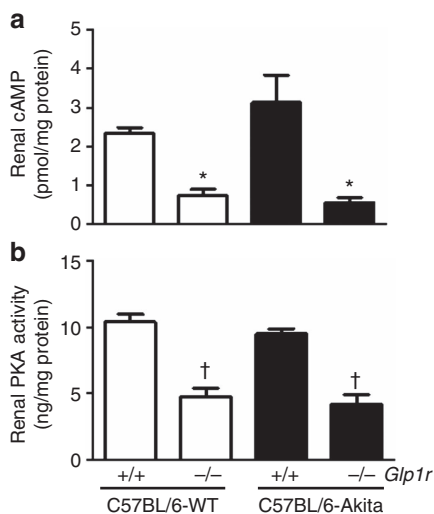


Figure 4 | Renal levels of cAMP and protein kinase A (PKA) activity in glucagon-like peptide-1 receptor (GLP-1R)-deficient C57BL/6-Akita mice. Renal levels of (a) cAMP and (b) PKA activity were determined in 30-week-old male mice ($n = 5$ per group; $*P < 0.01$, $†P < 0.001$ vs. *Glp1r*^{+/+} C57BL/6-WT). WT, wild type.

increasing renal oxidative stress in the setting of diabetes (Figure 5e). Recent experimental studies have reported that NAD(P)H oxidase NOX4 component is a major source of renal superoxide in the diabetic state,⁹ and that chronic

hyperglycemia enhances renal activity of NAD(P)H oxidase.^{10,23} Consistent with these findings, we observed that glomerular NOX4 expression and renal NAD(P)H oxidase activity were increased in C57BL/6-Akita diabetic mice relative to nondiabetic mice (Figure 5a, c and f).

Reduction of glomerular NO accelerates the progression of albuminuria and mesangial expansion in diabetic mice.^{24–26} Therefore, we examined glomerular NO levels by evaluation of the fluorescent intensity of the diamino-fluorescein-2 diacetate reaction. As shown in Figure 5a and d, C57BL/6-Akita diabetic mice showed decreased glomerular NO levels. Semiquantitative analysis of glomerular NO fluorescence intensity revealed significantly lower glomerular NO levels in diabetic *Glp1r*^{-/-} C57BL/6-Akita mice (Figure 5d). In contrast, there was no significant difference in glomerular NO levels between the two C57BL/6-WT nondiabetic mouse groups (Figure 5a and d).

Renal glomerular expression of fibrogenic cytokines in *Glp1r*^{-/-} C57BL/6-Akita mice

Thrombospondin-1 (TSP-1) is a homeotrimetric glycoprotein identified as an endogenous activator of transforming growth factor-β1 (TGF-β1).²⁷ TGF-β1 and connective tissue growth factor (CTGF) are well-known fibrogenic cytokines implicated in the development of renal hypertrophy and mesangial expansion in diabetic nephropathy.^{28,29} Hence, we

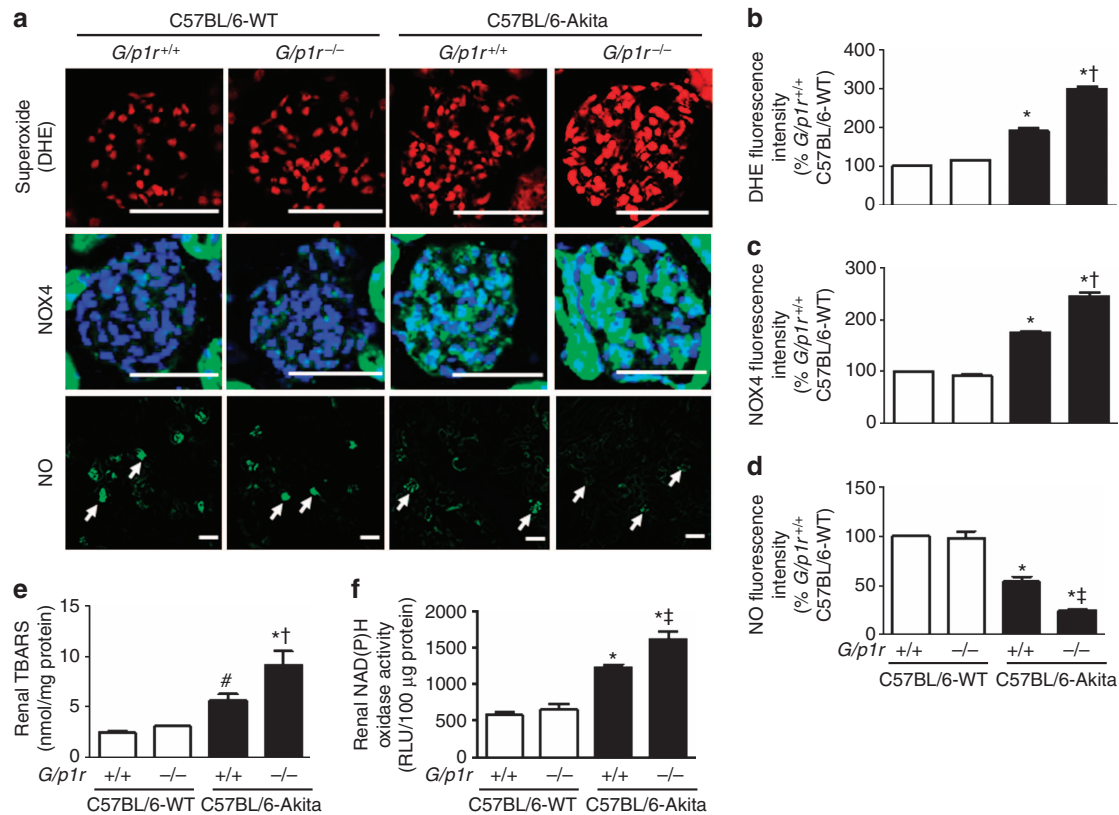


Figure 5 | Renal oxidative stress, NAD(P)H oxidase, and nitric oxide (NO) levels in glucagon-like peptide-1 receptor (GLP-1R)-deficient C57BL/6-Akita mice. (a) Representative images of glomerular dihydroethidium (DHE) staining, NOX4 immunohistochemistry, and *in situ* NO detection by diaminofluorescein-2 diacetate (DAF-2DA) perfusion method in 30-week-old male mouse kidneys. Arrows indicate glomerulus. Bars = 50 µm. Semiquantified fluorescence intensity of glomerular (b) DHE staining, (c) NOX4, and (d) NO were determined as described in Materials and Methods ($n = 5$ per group; * $P < 0.001$ vs. *Glp1r*^{+/+} C57BL/6-WT; † $P < 0.05$, ‡ $P < 0.01$ vs. *Glp1r*^{+/+} C57BL/6-Akita). Renal levels of (e) thiobarbituric acid-reactive substance (TBARS) and (f) NAD(P)H oxidase activity in 30-week-old male mice are shown in lower panels ($n = 5$ per group; * $P < 0.001$, # $P < 0.05$ vs. *Glp1r*^{+/+} C57BL/6-WT; † $P < 0.05$, ‡ $P < 0.01$ vs. *Glp1r*^{+/+} C57BL/6-Akita). RLU, relative chemiluminescence (light) unit; WT, wild type.

examined renal glomerular expression of TSP-1, TGF-β1, and CTGF in 30-week-old mice. Strikingly, *Glp1r*^{-/-} C57BL/6-Akita mice exhibited increased TSP-1 expression in glomerular capillary walls (Figure 6a and b) and significantly higher glomerular mRNA levels of TGF-β1 and CTGF (Figure 6c and d). In contrast, these glomerular changes were not observed in nondiabetic *Glp1r*^{+/+} C57BL/6-WT mice that displayed normal glomerular histology.

Effects of a GLP-1R agonist liraglutide on renal function, histological changes, and oxidative stress in DN-prone KK/Ta-Akita mice

We next assessed whether the activation of GLP-1R using the GLP-1R agonist liraglutide suppresses the progression of renal injury in KK/Ta-Akita mice, a mouse model of progressive DN.¹⁸ Mice were treated with liraglutide alone or in combination with an adenylate cyclase inhibitor SQ22536 or a selective PKA inhibitor H-89.

Table 2 shows physiological and biochemical data after a 4-week treatment period in 8-week-old KK/Ta-Akita mice. Although all groups of mice were similar with respect to body weight, systolic blood pressure, blood glucose, plasma insulin, blood urea nitrogen, plasma creatinine, and serum

lipids, mice treated with liraglutide alone exhibited lower levels of urinary albumin-to-creatinine ratio, GFR, and kidney weight. These results suggest that liraglutide attenuates the development of diabetic renal changes such as overt albuminuria, glomerular hyperfiltration, and renal hypertrophy without affecting the severity of diabetes and diabetes-related factors. Furthermore, SQ22536 and H-89 abolished the renal protective effects of liraglutide.

We next examined changes in renal histopathology, oxidative stress, NO, cAMP, and PKA activity after a 4-week treatment with liraglutide, with or without SQ22536 or H-89, in 8-week-old KK/Ta-Akita mice. As shown in Figure 7a (PAS staining) and 7b, moderate mesangial expansion was observed in vehicle-treated KK/Ta-Akita mice; however, mesangial expansion was reduced by liraglutide administration. FN accumulation in glomerular capillary walls was significantly diminished in the KK/Ta-Akita mice treated with liraglutide alone (Figure 7a and c). Furthermore, the KK/Ta-Akita mice treated with liraglutide alone exhibited higher podocyte number (Figure 7a and d) and lower GBM thickness (Figure 7a and e) than vehicle-treated KK/Ta-Akita mice. Notably, the amelioration of glomerular histopathological damage by liraglutide was eliminated in KK/Ta-Akita

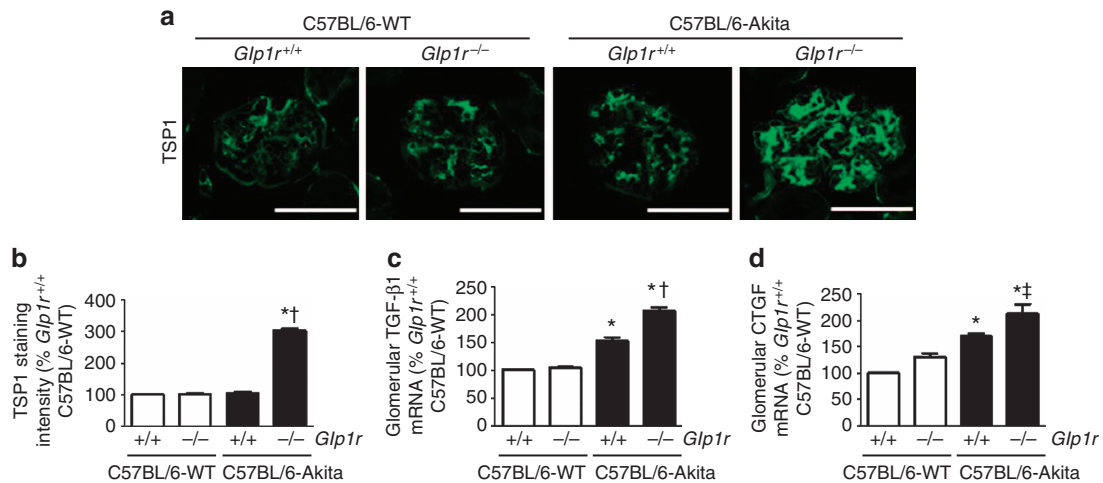


Figure 6 | Glomerular expression of thrombospondin-1 (TSP-1) and fibrogenic cytokines in glucagon-like peptide-1 receptor (GLP-1R)-deficient C57BL/6-Akita mice. (a) Representative images of glomerular TSP-1 immunohistochemistry in 30-week-old male mouse kidneys. Bars = 50 μm. (b) Semiquantified fluorescence intensity of glomerular TSP-1 (n = 5 per group; *P < 0.001 vs. *Glp1r*^{+/+} C57BL/6-WT; †P < 0.001 vs. *Glp1r*^{+/+} C57BL/6-Akita). Glomerular expression levels of (c) transforming growth factor-β1 (TGF-β1) and (d) connective tissue growth factor (CTGF) were determined by quantitative reverse transcriptase polymerase chain reaction (PCR) in 30-week-old male mice (n = 5 per group; *P < 0.001 vs. *Glp1r*^{+/+} C57BL/6-WT; †P < 0.01, ‡P < 0.05 vs. *Glp1r*^{+/+} C57BL/6-Akita). WT, wild type.

Table 2 | Physiological and biochemical parameters after a 4-week treatment with liraglutide either alone or in combination with SQ22536 or H-89 in male KK/Ta-Akita mice

Parameter	Vehicle	Liraglutide + SQ22536	Liraglutide + H-89	Liraglutide alone
n	6	6	6	6
BW (g)	21.5 ± 1.4	22.0 ± 0.5	22.6 ± 0.4	20.1 ± 0.7
SBP (mm Hg)	116 ± 3	112 ± 7	114 ± 4	115 ± 6
BG (mg/dl)	504 ± 41	481 ± 31	507 ± 39	492 ± 22
Plasma insulin (ng/ml)	0.06 ± 0.04	0.08 ± 0.02	0.07 ± 0.02	0.06 ± 0.05
BUN (mg/dl)	38.0 ± 1.4	40.3 ± 2.6	40.0 ± 2.6	32.2 ± 1.5
Cre (mg/dl)	0.94 ± 0.08	0.94 ± 0.08	0.95 ± 0.07	0.73 ± 0.04
TC (mg/dl)	136 ± 14	128 ± 10	122 ± 8	135 ± 4
TG (mg/dl)	229 ± 21	238 ± 20	272 ± 30	268 ± 20
ACR (μg/mg creatinine)	603 ± 56	618 ± 100	760 ± 84	201 ± 26*
GFR (μl/min/g BW)	16.4 ± 0.8	ND	ND	10.8 ± 1.1*
LKW/BW (g/kg)	14.9 ± 1.5	12.3 ± 0.5	12.1 ± 0.3	10.6 ± 0.5†

Abbreviations: ACR, urinary albumin-to-creatinine ratio; BG, blood glucose; BUN, blood urea nitrogen; BW, body weight; Cre, plasma creatinine; GFR, glomerular filtration rate; LKW, left kidney weight; SBP, systolic blood pressure; TC, total cholesterol; TG, triglyceride.

Values are means ± s.e.m.
*P < 0.01, †P < 0.05 vs. vehicle.

mice treated with liraglutide in combination with either SQ22536 or H-89.

Figure 8 shows renal cAMP and PKA activity levels in 8-week-old KK/Ta-Akita mice. KK/Ta-Akita mice treated with liraglutide alone for 4 weeks displayed higher renal levels of cAMP and PKA activity than vehicle-treated KK/Ta-Akita mice. In contrast, renal cAMP did not increase after treatment with SQ22536, and was only modestly increased in mice treated with H-89, whereas PKA activity levels were not increased in kidneys of KK/Ta-Akita mice treated with liraglutide in combination with SQ22536 or H-89.

Figure 9 shows the degree of renal oxidative stress and glomerular NO levels in 8-week-old KK/Ta-Akita mice. The treatment with liraglutide alone for 4 weeks significantly

reduced glomerular levels of superoxide and NOX4 expression and increased glomerular NO levels in KK/Ta-Akita mice (Figure 9a-d). Furthermore, we observed significant reduction of renal TBARS and NAD(P)H oxidase activity levels in the KK/Ta-Akita mice treated with liraglutide alone as compared with vehicle-treated KK/Ta-Akita mice (Figure 9e and f). In contrast, the renoprotective effects of liraglutide were abolished by coadministration of either SQ22536 or H-89.

DISCUSSION

The present study, using *in situ* hybridization and RT-PCR analyses, demonstrates that *Glp1r* mRNA transcripts are localized in glomerular capillary walls and throughout vascular walls, but not in tubules and collecting ducts, in the mouse kidney. More recently, Panjwani *et al.*²⁰ have demonstrated that commercially available widely used GLP-1R antisera are neither sensitive nor specific, and detect comparable immunoreactive bands in tissue extracts of both *Glp1r*^{+/+} and *Glp1r*^{-/-} mice.²⁰ Similar concerns surrounding the use of commercially available GLP-1R antisera have been raised by other groups.²¹ Hence, to avoid the pitfalls inherent in using antisera with suboptimal sensitivity and specificity, we used *in situ* hybridization and RT-PCR analysis to assess the expression and localization of *Glp1r* expression within the kidney.

To explore whether the presence or absence of GLP-1R signaling has a crucial role in the development and progression of DN, we disrupted the *Glp1r* gene in the DN-resistant mouse model C57BL/6-Akita and investigated its renal phenotype. The C57BL/6-Akita mice exhibit less oxidative and diabetic renal damage despite having relatively high renal activity of NAD(P)H oxidase, a major source of superoxide, because superoxide dismutase antioxidant

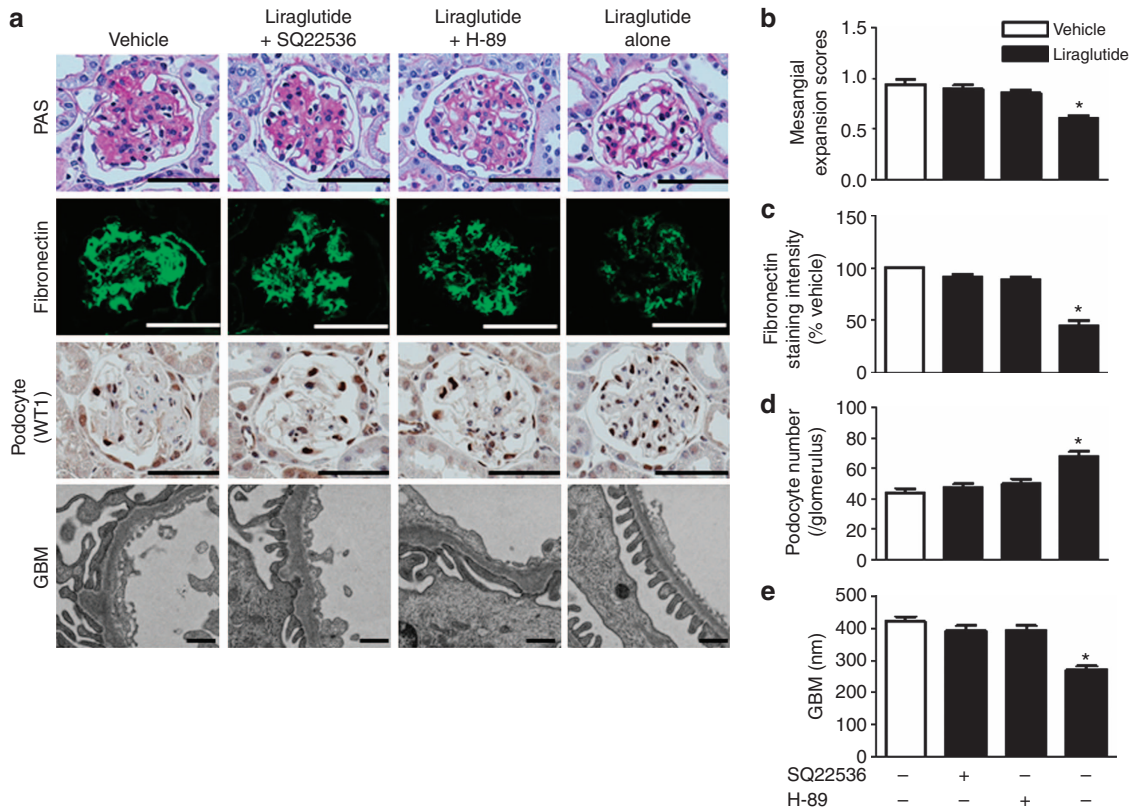


Figure 7 | Renal histopathology in liraglutide-treated KK/Ta-Akita mice. Treatment with liraglutide (200 µg/kg per day) either alone or in combination with SQ22536 or H-89 started at 8 weeks of age and ended at 12 weeks of age in male KK/Ta-Akita mice. (a) Representative glomerulus photomicrographs of periodic acid-Schiff (PAS) staining, fibronectin immunohistochemistry, WT1 staining, and electron microscopic analysis in the kidneys removed after a 4-week liraglutide treatment. Bars = 50 µm for PAS, fibronectin, and WT1 images or 1 µm for glomerular basement membrane (GBM) images. (b) Glomerular mesangial expansion scores. (c) Semiquantified fluorescence intensity of glomerular fibronectin. (d) The number of WT1-positive podocytes in glomeruli. (e) GBM thickness (n = 5 per group; *P < 0.001 vs. vehicle).

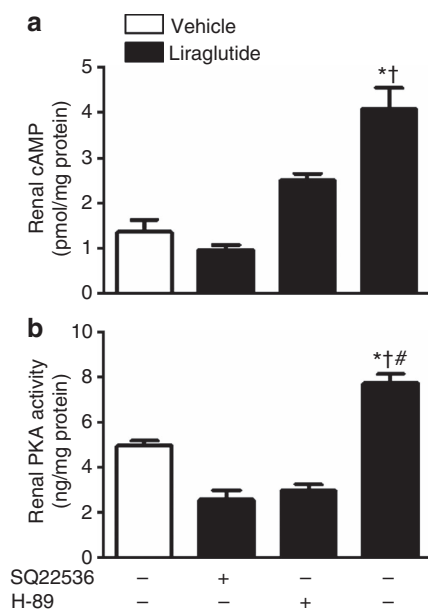


Figure 8 | Renal levels of cAMP and protein kinase A (PKA) activity in liraglutide-treated KK/Ta-Akita mice. Renal levels of (a) cAMP and (b) PKA activity were determined in 4-week liraglutide-treated mice (n = 5 per group; *P < 0.01 vs. vehicle; †P < 0.001 vs. SQ22536; ‡P < 0.001 vs. H-89).

defense system works well in their kidneys.¹⁸ Interestingly, the present data indicate that loss of the GLP-1R induces the upregulation of glomerular NOX4 expression and further elevation of renal NAD(P)H oxidase activity, resulting in elevation of glomerular superoxide and renal oxidative stress levels in the C57BL/6-Akita mice. These renal alterations secondary to GLP-1R deficiency contribute to the development of overt DN in the DN-resistant C57BL/6-Akita mice, as evidenced by pronounced mesangial expansion, podocyte reduction, and GBM thickening. Therefore, it is conceivable that loss of GLP-1 action resulting from GLP-1R deficiency directly reduces the renal antioxidant defense capacity against increased oxidative stress under hyperglycemic conditions. Furthermore, consistent with the lack of a significant islet phenotype arising in other insulin-resistant diabetic murine models lacking the *Glp1r* such as the *ob/ob Glp1r^{-/-}* mouse,³⁰ we found that GLP-1R deficiency does not affect insulin and GLP-1 secretion, glucose tolerance, islet topography, or other metabolic factors in the C57BL/6-Akita mice.

To further elucidate the mechanism underlying renal alterations observed in the *Glp1r^{-/-}* C57BL/6-Akita mice, we investigated renal cAMP-PKA, an important second

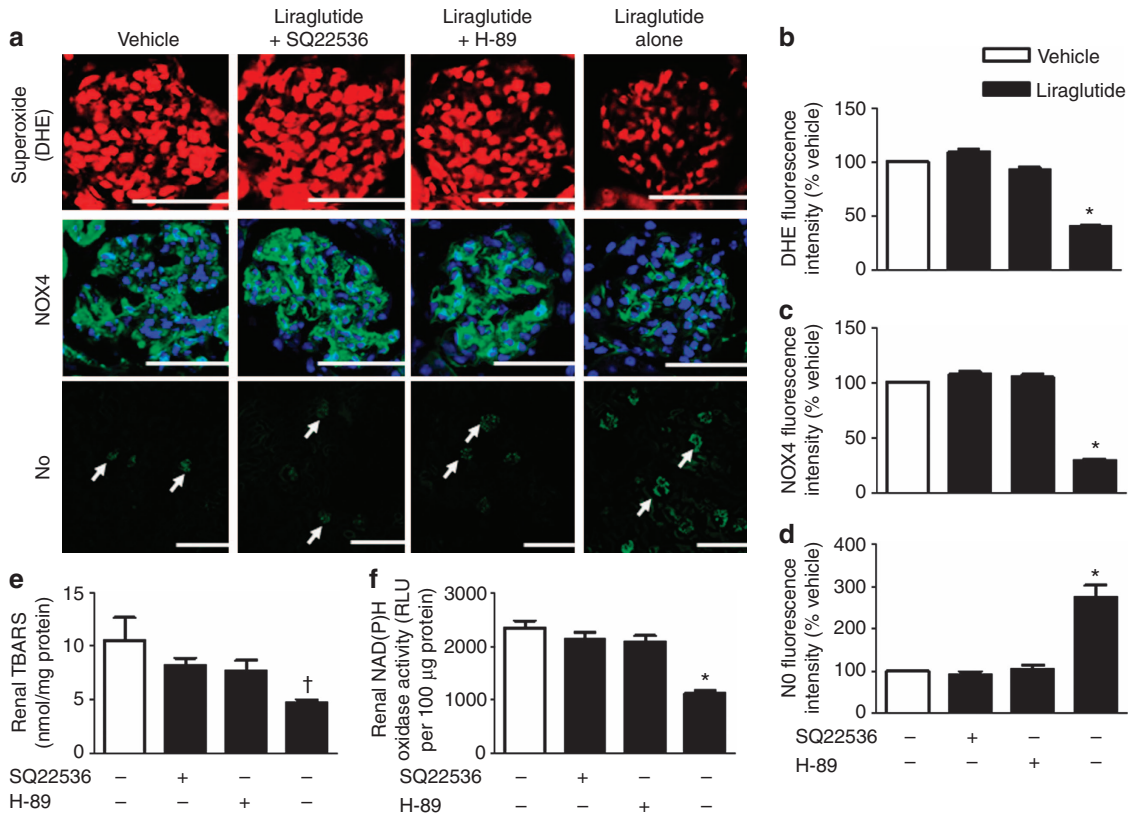


Figure 9 | Renal oxidative stress, NAD(P)H oxidase, and nitric oxide (NO) levels in liraglutide-treated KK/Ta-Akita mice. (a) Representative photomicrographs of glomerular dihydroethidium (DHE) staining, NOX4 immunohistochemistry, and *in situ* NO detection by diaminofluorescein-2 diacetate (DAF-2DA) perfusion method in 4-week liraglutide-treated mice. Arrows indicate glomerulus. Bars = 50 μm. Semiquantified fluorescence intensity of glomerular (b) DHE staining, (c) NOX4, and (d) NO were determined as described in Materials and Methods (n = 5 per group; *P < 0.001 vs. vehicle). Renal levels of (e) thiobarbituric acid-reactive substance (TBARS) and (f) NAD(P)H oxidase activity in 4-week liraglutide-treated mice are shown in lower panels (n = 5 per group; †P < 0.05, *P < 0.001 vs. vehicle). RLU, relative chemiluminescence (light) unit.

messenger system downstream of GLP-1R activation. Our results indicate that GLP-1R deficiency causes marked basal reduction of intrarenal cAMP formation and PKA activity in the C57BL/6-Akita mice. Given the evidence that cAMP and PKA represent important inhibitory factors for NAD(P)H oxidase,^{11,12,31,32} it is conceivable that *Glp1r*^{-/-} C57BL/6-Akita mice greatly increased their renal NAD(P)H oxidase activity owing to reduction of cAMP levels in the setting of chronic hyperglycemia, resulting in renal superoxide overproduction beyond their superoxide dismutase superoxide-scavenging capacity.

It is well known that oxidative stress upregulates fibrogenic cytokines such as TGF-β1 and CTGF, leading to mesangial cell proliferation and extracellular matrix production.^{29,33} Our study indicated that *Glp1r*^{-/-} C57BL/6-Akita mice have higher renal expression levels of TGF-β1 and CTGF in addition to TSP-1, an endogenous activator of TGF-β1. Hence, increased activity of these fibrogenic cytokines may contribute to the pronounced mesangial expansion observed in the *Glp1r*^{-/-} C57BL/6-Akita mice. Another interesting finding observed in the kidneys of *Glp1r*^{-/-} C57BL/6-Akita mice is glomerular NO reduction. Excessive superoxide anion could reduce glomerular NO levels by

scavenging NO from glomerular endothelial cells.^{34,35} NO is an important regulator for charge selectivity in the endothelial cell layer, and therefore glomerular NO reduction could enhance the permselectivity of plasma albumin through glomerular capillary wall. Arcos *et al.*³⁶ showed that chronic NO inhibition impairs glomerular charge selectivity barrier and causes albuminuria in rats. Furthermore, experimental studies of diabetic rats and mice indicated that renal NO reduction is associated with the development of renal histologic lesions,³⁷ and that NO deficiency by endothelial NO synthase knockout causes glomerular endothelial injury and overt albuminuria.²⁵ Taken together, it is plausible that glomerular NO reduction triggered by excessive oxidative stress contributed to increased albuminuria in *Glp1r*^{-/-} C57BL/6-Akita mice.

Recently, we generated a mouse model of progressive DN: KK/Ta-Akita. In contrast to C57BL/6-Akita mice, the KK/Ta-Akita mice show high susceptibility to DN, as evidenced by the development of severe albuminuria and prominent mesangial expansion.¹⁸ We reported that the diabetic renal changes in the KK/Ta-Akita mice are attributable to excessive renal oxidative stress.¹⁸ In this regard, the KK/Ta-Akita mouse represents a useful model to assess whether activation

of GLP-1R signaling suppresses the progression of DN *via* amelioration of renal oxidative stress. The present data clearly show that the GLP-1R agonist liraglutide ameliorates oxidative stress by elevating cAMP and PKA activity levels, downregulating NOX4, and reducing NAD(P)H oxidase activity in the kidneys of KK/Ta-Akita mice. Furthermore, liraglutide suppresses the progression of diabetic renal pathology, as evidenced by renal alterations such as reduced albuminuria, attenuated mesangial expansion, enhanced glomerular NO levels, and improved glomerular hyperfiltration and renal hypertrophy, in KK/Ta-Akita mice. It is noteworthy that renal improvement was induced without major changes in insulin secretion, glucose tolerance, and other metabolic factors. Collectively, these findings support the concept that GLP-1R signaling directly exerts antioxidative and protective effects on the hyperglycemic kidney. Furthermore, the beneficial actions of liraglutide were inhibited by the adenylate cyclase inhibitor SQ22536 and the selective PKA inhibitor H89, consistent with a critical role for cAMP and PKA-dependent pathways downstream of GLP-1R activation in renal protection. However, we cannot rule out the possibility that other signaling pathways may also be involved, given the possibility for 'off-target' inhibition when these and other inhibitors are used at high concentrations.

Consistent with the gain-of-function studies reported here, GLP-1R agonists such as exendin-4 and liraglutide attenuated diabetic renal injury, including mesangial expansion and albuminuria through the protection of glomerular endothelial cells,³⁸ reduction of renal oxidative stress,³⁹ and suppression of renal inflammatory cytokines⁴⁰ in high-dose streptozotocin (STZ)-induced diabetic rats and mice. However, there are several important differences in renal outcomes between our Akita mouse models and the STZ diabetic animals. Notably, albuminuria in the STZ rats is more severe than that in KK/Ta-Akita diabetic mice, exceeding 2.0 mg/24 h.^{39,40} Furthermore, STZ is known to induce nonspecific toxicity in multiple organs including kidney, liver, and arteries, especially when it is used at high doses.^{41,42} Therefore, it is likely that these deleterious effects of STZ caused greater kidney damage and more severe albuminuria in the STZ rats. More importantly, it has been shown that STZ stimulates superoxide production⁴³ and induces robust oxidative stress in the kidneys as compared with spontaneous diabetic mice.⁴⁴ In this context, our KK/Ta-Akita mouse model that develops overt DN without chemicals such as STZ or alloxan provides valuable information regarding the role of GLP-1R signaling in DN arising in the absence of chemically induced renal injury.

Finally, our data support a model for a GLP-1R-dependent intrarenal signaling pathway, as summarized in Figure 10. The present study provides the first evidence that loss of GLP-1R signaling upregulates renal NAD(P)H oxidase and increases renal oxidative stress, with reduced levels of renal cAMP-PKA activity in the setting of chronic hyperglycemia accentuating the progression of DN. Furthermore, the

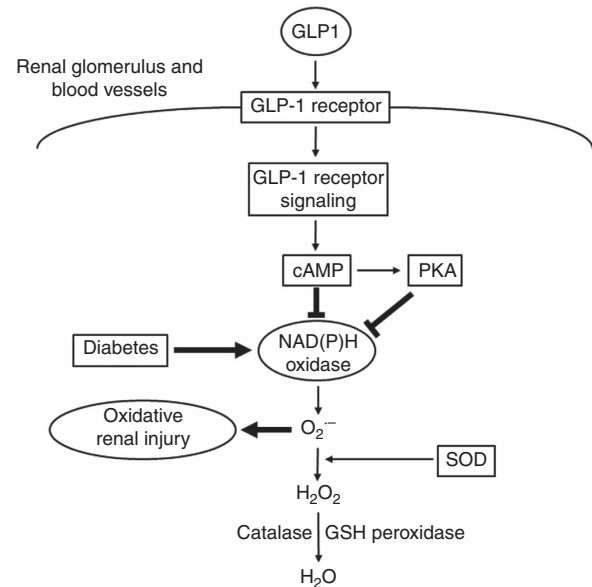


Figure 10 | Proposed glucagon-like peptide-1 receptor-dependent signal-transduction pathway in the kidney. Glucagon-like peptide-1 receptors are expressed in the glomerulus and blood vessels in the kidney. After glucagon-like peptide (GLP-1) binds to its receptor on glomerular capillary and vascular walls, glucagon-like peptide-1R signals upregulate the production of a major second messenger cAMP and consequently activate protein kinase A (PKA). The upregulated cAMP and PKA are expected to contribute to the amelioration of oxidative renal injury via inhibition of a major source of superoxide anion ($O_2^{\bullet -}$), NAD(P)H oxidase, activated under chronic diabetic condition. GSH, glutathione; H_2O_2 , hydrogen peroxide; SOD, superoxide dismutase.

present study illustrates that GLP-1R agonists suppress the progression of DN through antioxidative actions. These data support the concept of future clinical studies investigating whether renal outcomes will be similarly modified in subjects with diabetic kidney disease.

MATERIALS AND METHODS

Experimental animals and liraglutide treatment

C57BL/6-Akita mice are available from SLC (Hamamatsu, Shizuoka, Japan). The generation of *Glp1r*^{-/-} C57BL/6 mice has been described previously.⁴⁵ *Glp1r*^{-/-} C57BL/6-Akita mice were generated using C57BL/6-Akita and *Glp1r*^{-/-} C57BL/6 mice. Male C57BL/6-WT and C57BL/6-Akita mice with or without GLP-1R deficiency were used for the study. Biochemical and physiological parameters, renal histopathology, and renal oxidative stress markers were examined at 30 weeks of age in these mice. KK/Ta-Akita mice were generated as described previously.¹⁸ Eight-week-old male KK/Ta-Akita mice were subcutaneously injected with the GLP-1R agonist liraglutide (200 µg/kg per day; Novo Nordisk, Novo Alle, Bagsvaerd, Denmark) either alone or in combination with an adenylate cyclase inhibitor SQ22536 (2 mg/kg per day; Sigma-Aldrich, St Louis, MO) or a selective PKA inhibitor H-89 (2 mg/kg per day; Sigma-Aldrich) administered by retro-orbital injection under light isoflurane anesthesia for 4 weeks. A parallel group of control age-matched male KK/Ta-Akita mice was injected with an equivalent volume of the vehicle (saline). The mice were allowed unrestricted access to standard rodent chow and water. Animal experiments were carried out in accordance with the Animal

Welfare Guidelines of Akita University. All procedures were approved by the Committee on Animal Experimentation of Akita University.

Blood and urine parameters

Blood glucose was measured on samples obtained after a 6-h daytime fast using Glucocard Diameter (Arkray, Tokyo, Japan). Blood urea nitrogen, plasma creatinine, plasma total cholesterol, and plasma triglycerides were enzymatically measured using an auto-analyzer (Fuji Dry-Chem 5500; Fuji Film, Tokyo, Japan). Urinary albumin excretion was assessed by the determination of albumin-to-creatinine ratio on morning spot urine, as described previously.⁴⁶ Plasma active GLP-1 and insulin were determined using a GLP-1 (active) ELISA kit (Shibayagi, Gunma, Japan) and an insulin ELISA kit (Morinaga, Yokohama, Japan), respectively.

Physiological parameters

Systolic blood pressure was measured in conscious trained mice using a noninvasive tail cuff and pulse transducer system (BP-98A; Softron, Tokyo, Japan). GFR was measured by a single-bolus fluorescein isothiocyanate-inulin injection and clearance method, as described previously.⁴⁷

In situ hybridization

The sense and antisense riboprobes were directed against mouse *Glp1r* (bp 108–500; GenBank NM_021332) and generated by RT-PCR to amplify a 393-bp fragment. Detailed protocol for *in situ* hybridization is described in Supplementary Material online.

Isolation of glomeruli and quantitative RT-PCR

Glomeruli and tubuli were separated from the renal cortex of 8-week-old male C57BL/6-WT mice by Dynabead perfusion method as reported previously, with some modifications.⁴⁸ To further investigate the localization of *Glp1r* mRNA transcripts in the kidney in addition to *in situ* hybridization analysis, we performed RT-PCR analysis using total RNA extracted from glomeruli, tubuli, and renal arteries. Furthermore, RT-PCR analysis of glomerular TGF- β 1 and CTGF in addition to GLP-1R was performed at 30 weeks of age in male C57BL/6-WT and C57BL/6-Akita mice with or without GLP-1R deficiency, as described previously.¹⁹

Histologic analysis

The kidneys were perfused via the left ventricle with phosphate-buffered saline, followed by 4% paraformaldehyde in phosphate-buffered saline, removed, and fixed in 4% paraformaldehyde in phosphate-buffered saline overnight at 4 °C. Two- μ m-thick paraffin sections were stained with PAS. A semiquantitative score was used to evaluate the degree and extent of glomerular mesangial expansion, as described previously.¹⁸ Podocyte number was evaluated by WT1 immunohistochemistry and calculated using the Weibel-Gomez method, as reported previously.^{49,50} Five mice per group were analyzed, and more than 60 cortical glomeruli were assessed in each mouse. The thickness of GBM was evaluated by electron microscopic examination in five mice per group, as described previously.¹⁸

Immunofluorescence histochemistry, DHE histochemistry, and in situ NO detection

Histochemical analysis was performed as described previously.^{5,18,19,51} Five mice per group were analyzed, and more than 20 cortical glomeruli were assessed in each mouse. Detailed protocols

for immunofluorescence histochemistry, DHE histochemistry, and *in situ* NO detection are described in Supplementary Material online.

Measurement of renal cAMP and PKA activity levels

Kidney lysate was prepared using phosphate-buffered saline-perfused and freshly removed renal cortical tissue, as described previously.¹⁸ Renal cAMP and PKA activity levels were measured in these kidney lysate samples using a DetectX Direct cAMP Immunoassay kit (Arbor Assays, Ann Arbor, MI) and a PKA kinase activity kit (Enzo Life Sciences, Farmingdale, NY), respectively. The levels were expressed as renal cortical cAMP and PKA activity to protein ratio.

Measurement of renal TBARS and NAD(P)H oxidase activity

Renal TBARS levels were measured in renal cortical tissue lysate samples using a TBARS assay kit (Cayman Chemical, Ann Arbor, MI). The levels were expressed as renal cortical TBARS to protein ratio. Renal NAD(P)H oxidase activity was measured in the same samples using a lucigenin-enhanced chemiluminescence assay, as described previously.¹⁰ Enzymatic activity of NAD(P)H was expressed in relative chemiluminescence (light) units (RLU) per 100 μ g of protein.

Statistical analysis

All data were presented as means \pm s.e.m. Statistical analysis of the data was performed using the GraphPad Prism software (GraphPad, San Diego, CA). Differences between multiple groups were determined by one-way analysis of variance followed by Bonferroni's multiple comparison test.

DISCLOSURE

DJD receives research support for cardiovascular studies from, and is a consultant to, Novo Nordisk, the manufacturer of liraglutide. All the other authors declared no competing interests.

ACKNOWLEDGMENTS

This work was supported by a Grant-in-Aid for Scientific Research (no. 20590943 to HF) from the Ministry of Education, Science and Culture of Japan and by the Canada Research Chairs Program (to DJD).

SUPPLEMENTARY MATERIAL

The protective roles of GLP-1R signaling in diabetic nephropathy: possible mechanism and therapeutic potential
Supplementary material is linked to the online version of the paper at <http://www.nature.com/ki>

REFERENCES

1. Brownlee M. The pathobiology of diabetic complications: a unifying mechanism. *Diabetes* 2005; **54**: 1615–1625.
2. Forbes JM, Coughlan MT, Cooper ME. Oxidative stress as a major culprit in kidney disease in diabetes. *Diabetes* 2008; **57**: 1446–1454.
3. Fujita H, Sakamoto T, Komatsu K *et al.* Reduction of circulating superoxide dismutase activity in type 2 diabetic patients with microalbuminuria and its modulation by telmisartan therapy. *Hypertens Res* 2011; **34**: 1302–1308.
4. Guzik TJ, Mussa S, Gastaldi D *et al.* Mechanisms of increased vascular superoxide production in human diabetes mellitus: role of NAD(P)H oxidase and endothelial nitric oxide synthase. *Circulation* 2002; **105**: 1656–1662.
5. Satoh M, Fujimoto S, Haruna Y *et al.* NAD(P)H oxidase and uncoupled nitric oxide synthase are major sources of glomerular superoxide in rats with experimental diabetic nephropathy. *Am J Physiol Renal Physiol* 2005; **288**: F1144–F1152.

6. Soccio M, Toniato E, Evangelista V *et al.* Oxidative stress and cardiovascular risk: the role of vascular NAD(P)H oxidase and its genetic variants. *Eur J Clin Invest* 2005; **35**: 305–314.
7. Wardle EN. Cellular oxidative processes in relation to renal disease. *Am J Nephrol* 2005; **25**: 13–22.
8. Fujita H, Fujishima H, Morii T *et al.* Modulation of renal superoxide dismutase by telmisartan therapy in C57BL/6-Ins2(Akita) diabetic mice. *Hypertens Res* 2012; **35**: 213–220.
9. Gorin Y, Block K, Hernandez J *et al.* Nox4 NAD(P)H oxidase mediates hypertrophy and fibronectin expression in the diabetic kidney. *J Biol Chem* 2005; **280**: 39616–39626.
10. Kitada M, Koya D, Sugimoto T *et al.* Translocation of glomerular p47phox and p67phox by protein kinase C-beta activation is required for oxidative stress in diabetic nephropathy. *Diabetes* 2003; **52**: 2603–2614.
11. Kim JS, Diebold BA, Babior BM *et al.* Regulation of Nox1 activity via protein kinase A-mediated phosphorylation of NoxA1 and 14-3-3 binding. *J Biol Chem* 2007; **282**: 34787–34800.
12. Saha S, Li Y, Anand-Srivastava MB. Reduced levels of cyclic AMP contribute to the enhanced oxidative stress in vascular smooth muscle cells from spontaneously hypertensive rats. *Can J Physiol Pharmacol* 2008; **86**: 190–198.
13. Baggio LL, Drucker DJ. Biology of incretins: GLP-1 and GIP. *Gastroenterology* 2007; **132**: 2131–2157.
14. Holz GG. Epac: a new cAMP-binding protein in support of glucagon-like peptide-1 receptor-mediated signal transduction in the pancreatic beta-cell. *Diabetes* 2004; **53**: 5–13.
15. Leech CA, Chepurny OG, Holz GG. Epac2-dependent rap1 activation and the control of islet insulin secretion by glucagon-like peptide-1. *Vitam Horm* 2010; **84**: 279–302.
16. Hirata K, Kume S, Araki S *et al.* Exendin-4 has an anti-hypertensive effect in salt-sensitive mice model. *Biochem Biophys Res Commun* 2009; **380**: 44–49.
17. Bullock BP, Heller RS, Habener JF. Tissue distribution of messenger ribonucleic acid encoding the rat glucagon-like peptide-1 receptor. *Endocrinology* 1996; **137**: 2968–2978.
18. Fujita H, Fujishima H, Chida S *et al.* Reduction of renal superoxide dismutase in progressive diabetic nephropathy. *J Am Soc Nephrol* 2009; **20**: 1303–1313.
19. Fujita H, Fujishima H, Takahashi K *et al.* SOD1, but not SOD3, deficiency accelerates diabetic renal injury in C57BL/6-Ins2(Akita) diabetic mice. *Metabolism* 2012; **61**: 1714–1724.
20. Panjwani N, Mulvihill EE, Longuet C *et al.* GLP-1 receptor activation indirectly reduces hepatic lipid accumulation but does not attenuate development of atherosclerosis in diabetic male ApoE(–/–) mice. *Endocrinology* 2013; **154**: 127–139.
21. Pyke C, Knudsen LB. The glucagon-like peptide-1 receptor—or not? *Endocrinology* 2013; **154**: 4–8.
22. Van Vliet A, Baelde HJ, Vleming LJ *et al.* Distribution of fibronectin isoforms in human renal disease. *J Pathol* 2001; **193**: 256–262.
23. Thallas-Bonke V, Thorpe SR, Coughlan MT *et al.* Inhibition of NADPH oxidase prevents advanced glycation end product-mediated damage in diabetic nephropathy through a protein kinase C-alpha-dependent pathway. *Diabetes* 2008; **57**: 460–469.
24. Zhao HJ, Wang S, Cheng H *et al.* Endothelial nitric oxide synthase deficiency produces accelerated nephropathy in diabetic mice. *J Am Soc Nephrol* 2006; **17**: 2664–2669.
25. Kanetsuna Y, Takahashi K, Nagata M *et al.* Deficiency of endothelial nitric-oxide synthase confers susceptibility to diabetic nephropathy in nephropathy-resistant inbred mice. *Am J Pathol* 2007; **170**: 1473–1484.
26. Wang CH, Li F, Hiller S *et al.* A modest decrease in endothelial NOS in mice comparable to that associated with human NOS3 variants exacerbates diabetic nephropathy. *Proc Natl Acad Sci USA* 2011; **108**: 2070–2075.
27. Daniel C, Schaub K, Amann K *et al.* Thrombospondin-1 is an endogenous activator of TGF-beta in experimental diabetic nephropathy *in vivo*. *Diabetes* 2007; **56**: 2982–2989.
28. Reeves WB, Andreoli TE. Transforming growth factor beta contributes to progressive diabetic nephropathy. *Proc Natl Acad Sci USA* 2000; **97**: 7667–7669.
29. Elmarakby AA, Sullivan JC. Relationship between oxidative stress and inflammatory cytokines in diabetic nephropathy. *Cardiovasc Ther* 2010; **30**: 49–59.
30. Scrocchi LA, Hill ME, Saleh J *et al.* Elimination of glucagon-like peptide 1R signaling does not modify weight gain and islet adaptation in mice with combined disruption of leptin and GLP-1 action. *Diabetes* 2000; **49**: 1552–1560.
31. Bengis-Garber C, Gruener N. Protein kinase A downregulates the phosphorylation of p47 phox in human neutrophils: a possible pathway for inhibition of the respiratory burst. *Cell Signal* 1996; **8**: 291–296.
32. Savitha G, Salimath BP. Cross-talk between protein kinase C and protein kinase A down-regulates the respiratory burst in polymorphonuclear leukocytes. *Cell Signal* 1993; **5**: 107–117.
33. Ohshiro Y, Ma RC, Yasuda Y *et al.* Reduction of diabetes-induced oxidative stress, fibrotic cytokine expression, and renal dysfunction in protein kinase C-beta-null mice. *Diabetes* 2006; **55**: 3112–3120.
34. Evans JL, Goldfine ID, Maddux BA *et al.* Oxidative stress and stress-activated signaling pathways: a unifying hypothesis of type 2 diabetes. *Endocr Rev* 2002; **23**: 599–622.
35. Forstermann U, Munzel T. Endothelial nitric oxide synthase in vascular disease: from marvel to menace. *Circulation* 2006; **113**: 1708–1714.
36. Arcos MI, Fujihara CK, Sesso A *et al.* Mechanisms of albuminuria in the chronic nitric oxide inhibition model. *Am J Physiol Renal Physiol* 2000; **279**: F1060–F1066.
37. Prabhakar S, Starnes J, Shi S *et al.* Diabetic nephropathy is associated with oxidative stress and decreased renal nitric oxide production. *J Am Soc Nephrol* 2007; **18**: 2945–2952.
38. Mima A, Hiraoka-Yamamoto J, Li Q *et al.* Protective effects of GLP-1 on glomerular endothelium and its inhibition by PKCbeta activation in diabetes. *Diabetes* 2012; **61**: 2967–2979.
39. Hendarto H, Inoguchi T, Maeda Y *et al.* GLP-1 analog liraglutide protects against oxidative stress and albuminuria in streptozotocin-induced diabetic rats via protein kinase A-mediated inhibition of renal NAD(P)H oxidases. *Metabolism* 2012; **61**: 1422–1434.
40. Kodera R, Shikata K, Kataoka HU *et al.* Glucagon-like peptide-1 receptor agonist ameliorates renal injury through its anti-inflammatory action without lowering blood glucose level in a rat model of type 1 diabetes. *Diabetologia* 2011; **54**: 965–978.
41. Breyer MD, Bottinger E, Brosius FC 3rd *et al.* Mouse models of diabetic nephropathy. *J Am Soc Nephrol* 2005; **16**: 27–45.
42. Inada A, Kanamori H, Arai H *et al.* A model for diabetic nephropathy: advantages of the inducible cAMP early repressor transgenic mouse over the streptozotocin-induced diabetic mouse. *J Cell Physiol* 2008; **215**: 383–391.
43. Szkudelski T. The mechanism of alloxan and streptozotocin action in B cells of the rat pancreas. *Physiol Res* 2001; **50**: 537–546.
44. Lubec B, Hermon M, Hoeger H *et al.* Aromatic hydroxylation in animal models of diabetes mellitus. *FASEB J* 1998; **12**: 1581–1587.
45. Hansotia T, Baggio LL, Delmeire D *et al.* Double incretin receptor knockout (DIRKO) mice reveal an essential role for the enteroinsular axis in transducing the glucoregulatory actions of DPP-IV inhibitors. *Diabetes* 2004; **53**: 1326–1335.
46. Qi Z, Fujita H, Jin J *et al.* Characterization of susceptibility of inbred mouse strains to diabetic nephropathy. *Diabetes* 2005; **54**: 2628–2637.
47. Qi Z, Whitt I, Mehta A *et al.* Serial determination of glomerular filtration rate in conscious mice using FITC-inulin clearance. *Am J Physiol Renal Physiol* 2004; **286**: F590–F596.
48. Takemoto M, Asker N, Gerhardt H *et al.* A new method for large scale isolation of kidney glomeruli from mice. *Am J Pathol* 2002; **161**: 799–805.
49. Tanabe K, Lanaspas MA, Kitagawa W *et al.* Nicorandil as a novel therapy for advanced diabetic nephropathy in the eNOS-deficient mouse. *Am J Physiol Renal Physiol* 2012; **302**: F1151–F1160.
50. Nicholas SB, Basgen JM, Sinha S. Using stereologic techniques for podocyte counting in the mouse: shifting the paradigm. *Am J Nephrol* 2011; **33**(Suppl 1): 1–7.
51. Fujita H, Kakei M, Fujishima H *et al.* Effect of selective cyclooxygenase-2 (COX-2) inhibitor treatment on glucose-stimulated insulin secretion in C57BL/6 mice. *Biochem Biophys Res Commun* 2007; **363**: 37–43.

Supplementary material

MATERIALS AND METHODS

In situ hybridization

The sense and antisense riboprobes were directed against mouse *Glp1r* (bp 108-500; GenBank NM_021332) and generated by RT-PCR to amplify a 393-bp fragment. Eight-week-old male C57BL/6-WT mice were anesthetized by an intraperitoneal injection of pentobarbital sodium (50 mg/kg body wt), and the kidneys were removed, fixed overnight in 4% paraformaldehyde at 4 °C, and embedded in paraffin. The kidney sections (6 µm) were deparaffinized, refixed in 4% paraformaldehyde, treated with proteinase K (20 µg/ml), washed with PBS, refixed in 4% paraformaldehyde, and treated with 0.1M triethanolamine plus 0.25% acetic anhydride. After washed with PBS, the kidney sections were dehydrated in 100% ethanol. The riboprobes (300 ng/ml) were hybridized to the sections at 60°C for 16 h. After hybridization, the sections were washed in 5× SSC at 50 °C for 20 min, 50% formamide at 50 °C for 20 min, and 2× SSC at 50 °C for 20 min, followed by the treatment with RNase (50 µg/ml) in 10 mM Tris-HCl (pH 8.0), 1mM EDTA and 1M NaCl at 37 °C for 30 min. Then the sections were washed twice in 2× SSC at 50 °C for 20 min, twice in 0.2× SSC at 50 °C for 20 min, and once in 0.1% Tween 20 in TBS (TBST). After the treatment with 0.5% blocking reagent (Roche Applied Science, Indianapolis, IN) in TBST for 30 min, the sections were incubated with anti-DIG AP conjugate (Roche) diluted 1:1000 with TBST for 2 h. The sections were washed twice in TBST and incubated in 100mM NaCl, 50 mM MgCl₂, 0.1% Tween 20, 100 mM Tris-HCl (pH 9.5). Coloring reactions were performed with NBT/BCIP solution (Sigma-Aldrich) overnight and then washed with PBS. The sections were counterstained with Kernechtrot stain solution (Muto Pure Chemicals, Tokyo, Japan) and the images were taken using NanoZoomer microscope (Hamamatsu Photonics,

Hamamatsu, Shizuoka, Japan).

Immunofluorescence histochemistry, DHE histochemistry, and *in situ* NO detection

Histochemical analysis was performed as described previously.¹⁻⁴ For insulin immunohistochemistry, cryostat pancreas sections were labeled with guinea pig anti-insulin antibody (1:100; DakoCytomation, Glostrup, Denmark), and then incubated with Alexa Fluor 488-conjugated goat anti-guinea pig IgG antibody (1:100; Molecular Probes, Eugene, OR). For fibronectin, TSP-1, and NOX-4 IHC, Cryostat kidney sections were labeled with mouse anti-fibronectin monoclonal antibody (1:100; Thermo Scientific, Fremont, CA), mouse anti-TSP-1 monoclonal antibody (1:100; Invitrogen, Camarillo, CA), or goat anti-NOX4 polyclonal antibody (1:100; Santa Cruz Biotechnology, Santa Cruz, CA), followed by Alexa Fluor 488-conjugated goat anti-mouse IgG antibody (1:200; Molecular Probes) or Alexa Fluor 488-conjugated donkey anti-goat IgG antibody (1:200; Molecular Probes). Then we counterstained the sections with 4',6-diamidino-2-phenylindole (DAPI; Molecular Probes). To assess glomerular superoxide levels, DHE histochemistry was performed as described previously.² Intracellular NO production in the glomeruli was assessed as reported previously.^{1,3} Fluorescent images were taken using confocal laser microscopy (LSM510; Carl Zeiss, Jena, Germany). The fluorescence intensity of glomeruli was semiquantified using Adobe Photoshop (version CS5; Adobe systems, San Jose, CA). Five mice per group were analyzed, and more than twenty cortical glomeruli were assessed in each mouse.

REFERENCES

1. Satoh M, Fujimoto S, Haruna Y, *et al.* NAD(P)H oxidase and uncoupled nitric oxide synthase are major sources of glomerular superoxide in rats with experimental diabetic nephropathy. *Am J Physiol Renal Physiol* 2005; **288**: F1144-1152.

2. Fujita H, Fujishima H, Chida S, *et al.* Reduction of renal superoxide dismutase in progressive diabetic nephropathy. *J Am Soc Nephrol* 2009; **20**: 1303-1313.
3. Fujita H, Fujishima H, Takahashi K, *et al.* SOD1, but not SOD3, deficiency accelerates diabetic renal injury in C57BL/6-Ins2(Akita) diabetic mice. *Metabolism* 2012; **61**: 1714-1724.
4. Fujita H, Kakei M, Fujishima H, *et al.* Effect of selective cyclooxygenase-2 (COX-2) inhibitor treatment on glucose-stimulated insulin secretion in C57BL/6 mice. *Biochem Biophys Res Commun* 2007; **363**: 37-43.